

ADI After Austenitising From Intercritical Temperature

A. Kowalski^{a*}, S. Kloska-Nawarecka^a, K. Regulski^b

^a Foundry Research Institute, Zakopiańska str. 73., 30-418 Krakow, Poland

^b AGH – University of Science and Technology, Mickiewicza str. Krakow, Poland

*Corresponding author. E-mail address: awkowal@poczta.fm

Received 18.07.2012; accepted in revised form 04.09.2012

Abstract

ADI subjected to austenitising at intercritical temperatures contains in its matrix the precipitates of pre-eutectoid ferrite. Studies were carried out on the ductile iron of the following chemical composition: C = 3,80%, Si = 2,30%, Mn = 0,28%, P = 0,060%, S = 0,010%, Mg = 0,065%, Ni = 0,60%, Cu = 0,70%, Mo = 0,21% This cast iron was austenitised at three different temperatures, i.e. 800, 815 and 830°C and austempered at 360 and 380°C. For each variant of the cast iron heat treatment, the mechanical properties, i.e. YS, TS, EL and Hardness, were measured, and structure of the matrix was examined. Higher plastic properties were obtained owing to the presence of certain amount of pre-eutectoid ferrite. The properties were visualised using fuzzy logic model in a MATLAB. software.

Keywords: Ductile cast iron, Austempering, Microstructure, Mechanical properties, Fuzzy logic

1. Introduction

The operation of austempering consists of two treatments following directly each other:

- austenitising, and
- austempering

When the austenitising temperature is too low, the pre-eutectoid coarse ferrite remains in the state of equilibrium with austenite and graphite. At this temperature, the complete austenitising treatment cannot be achieved, regardless of the holding time. The phase equilibrium diagram of an iron – graphite system is shown in Figure 1 in a binary system formed by the intersection of a ternary Fe-C-Si system at 2.5% Si. Within the temperature range in which a eutectic is present in the Fe-Cu alloys, a ternary Fe-C-Si system has a triple area in which ferrite, austenite and graphite co-exist. This area defines the lower critical temperature (LCT) and upper critical temperature (UCT) at which

austenite is formed during heating, or ferrite during cooling within of this range vary greatly with the addition of alloying elements.

According to [1], the temperature of the eutectoid transformation T_S for a stable Fe-C system can be calculated from the following empirical equation:

$$T_S = 738 + 35 \text{ Si} + 200 \text{ W} + 8 \text{ Cr} - 20 \text{ Ni} - 35 (n - 1,7 \text{ S}) - 10 \text{ Cu}, ^\circ\text{C} \quad (1)$$

Sikora et al. [4] developed an equation to calculate the upper critical temperature T_{c_u} for ductile iron:

$$T_{c_u} = 723 - 0,3 \text{ C} + 43 \text{ Si} - 33 \text{ Mn} - 6 \text{ Cu}, ^\circ\text{C} \quad (2)$$

This equation is applicable to cast iron of the following chemical composition: 2.70 <% C <3.80, 1.50 <% Si <3.70, 0.50 <% Cu <1.75, 0.50 <% Mn <1.10

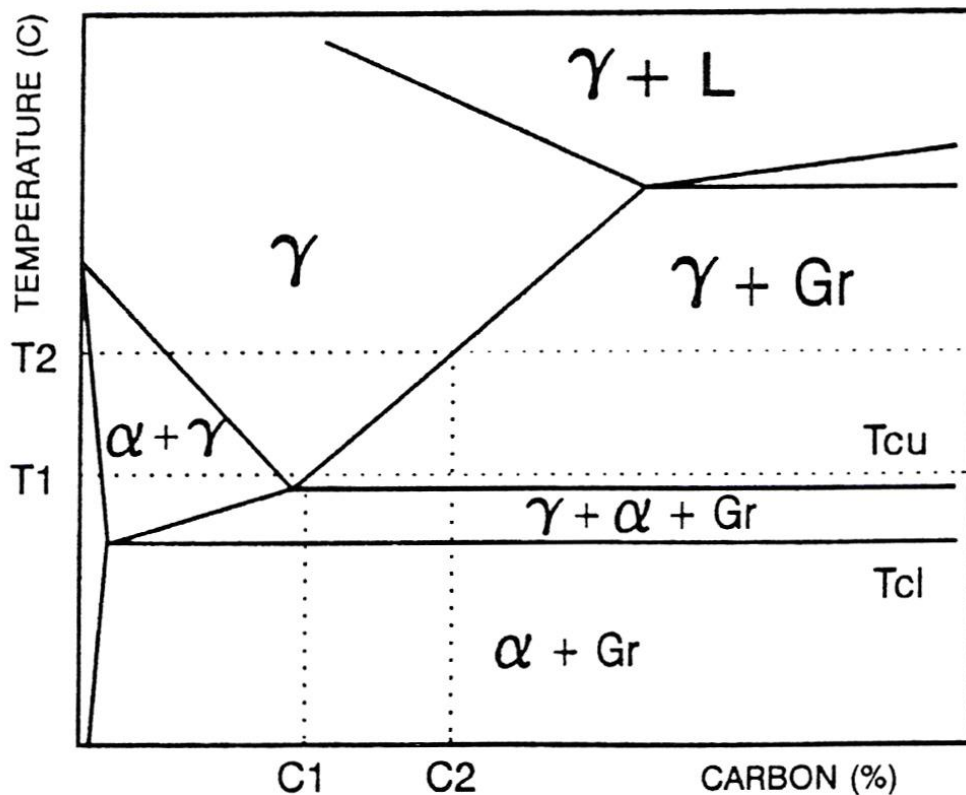


Fig. 1. Qualitative 2 D image of the phase equilibrium diagram for a ternary Fe-C-Si system containing 2,5% Si. γ – austenite, α – ferrite, G – graphite, T_{cu} – upper critical austenitising temperature, T_{cl} – lower critical austenitising temperature [4]

The temperature of the austenitising treatment should be selected in such a way as to make the individual values occur within the austenite + graphite ($\gamma + G$) phase field. Silicon increases the upper critical temperature, while manganese reduces this value. If the austenitising temperature is in the subcritical range ($\alpha + \gamma + G$) below the lower critical temperature, the matrix will contain pre-eutectoid ferrite

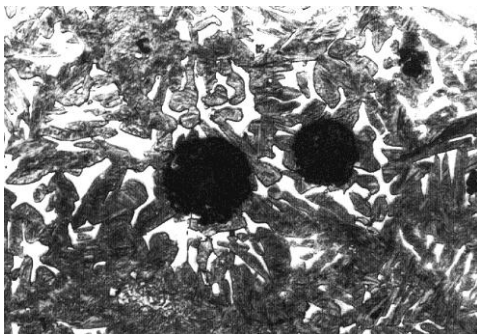


Fig. 2. Pre-eutectoid ferrite (bright, sharp outlined fields) in the structure of ADI after austenitising at 815 °C for 2 h and rapid cooling in water, 400x [2]

This effect was used to conduct the intentional partial austenitisation to get in the matrix after austempering a mixture of

(Fig. 1) [4]. The result of this phenomenon is the reduced strength and hardness of the casting.

Ferrite of this type is shown in Fig 2 [2]. It is easy to note that the largest concentration of ferrite grains occurs close to the spheroids of graphite, where the concentration of silicon is the highest. In these areas, the upper critical temperature assumes the highest values, too.

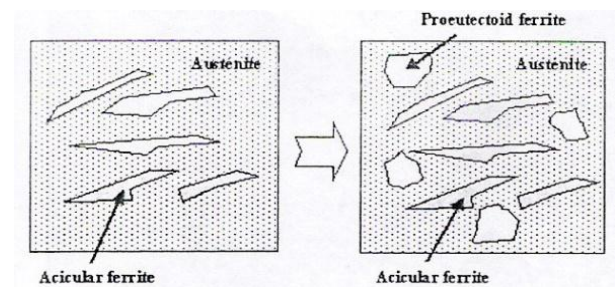


Fig. 3. Schematic diagram of a mixture of pre-eutectoid ferrite, acicular (lamellar) ferrite and austenite [5]

ferrite and pre-eutectoid ausferrite [3,5]. Cast iron of this type is characterised by a reduced strength and hardness, but offers much

higher ductility and toughness. An indisputable advantage of this cast iron is very good machinability, which allows machining of castings after heat treatment. For example, in the study [6], the following properties were obtained: TS = 700 MPa, YS = 500 MPa, EL = 14.5%, Hardness = 250, IS = 11 J/cm². To achieve the desired structure, the base cast iron must first undergo the operation of ferritisation. Thus, the heat treatment of this cast iron should take the following course:

ferritising + partial austenitising + high temperature austempering (350 - 380⁰ C).

This cast iron grade is known in the literature as FADI (Ferritic-Ausferritic Ductile Iron) or IADI (Intercritically Austenitised ADI). IADI grades have already been included in some international standards, to mention the 800-500-10 grade in ISO 17 804: 2005, and the 750-500-11 grade in SAE J2477: 2004 and ASTM A897/A897M: 2006.

Cast iron of this grade is particularly suitable for elements that require tight tolerances and very exact machining in austempered condition. In the United States, the 800-10 grade is believed to be an upgraded variation of the traditional ferritic ductile iron of grade 4512 [7]. With the strength nearly two times higher, castings can be designed with thinner walls, which will significantly reduce their weight.

2. Experimental procedure

Tests were carried out on ductile iron samples of the following chemical composition:

C = 3,80%, Si = 2,30%, Mn = 0,28%, P = 0,060%, S = 0,010%, Mg = 0,065%, Ni = 0,60%, Cu = 0,70%, Mo = 0,21%

The heat treatment (austempering) was carried out according to the cycles given in Table 1.

Table 1.

Heat treatment variants during partial austenitising

Cycle	Austeni-tising	Austem-pering
1	800	360
2	815	360
3	830	360
4	800	380
5	815	380
6	830	380

In each cycle the holding time was 1h

3. Results and discussion

Pre-eutectoid ferrite was obtained in an amount of 5 to 15%. Examples of microstructure are shown in Figs. 4 -9.

Table 2.

Mechanical properties of ADI after partial austenitising

No.	Cycle	Mechanical properties					Microstructure of metallic matrix
		YS, MPa	TS, MPa	EL, %	Pct RE, %	Hardness HRC	
1	1	920	1041	5,6	9,2	36	Lower ausferrite + pre-eutectoid ferrite + austenite + martensite (traces)
2	2	901	1037	6,0	9,1	37	
3	3	915	1045	6,9	7,6	37	
4	4	821	986	10,4	9,8	34	
5	5	766	919	7,9	8,9	34	
6	6	806	969	8,3	7,9	35	



Fig. 4. Microstructure of ADI from C1 cycle. Etched with Beraha reagent - Martensite, 1000x. Pre-eutectoid ferrite, lower bainite, austenite

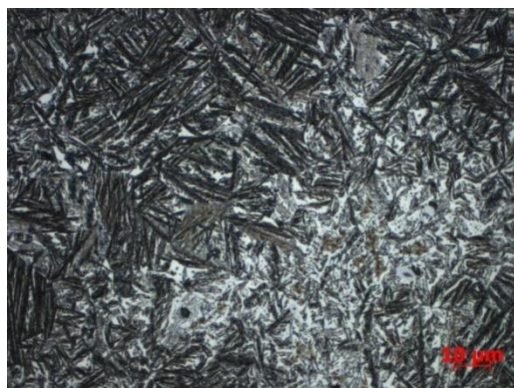


Fig. 5. Microstructure of ADI from C2 cycle. Etched with Beraha reagent - Martensite, 1000x. Pre-eutectoid ferrite, lower bainite, austenite

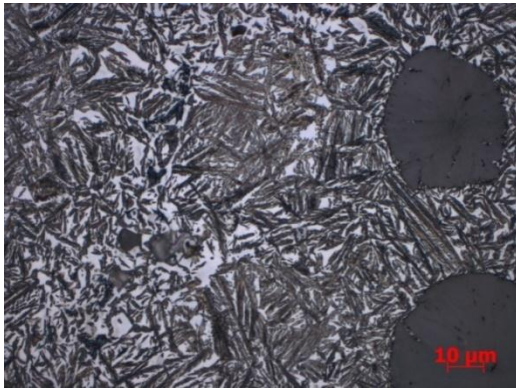


Fig. 6. Microstructure of ADI from C3 cycle. Etched with Beraha reagent - Martensite, 1000x. Pre-eutectoid ferrite, lower bainite, austenite

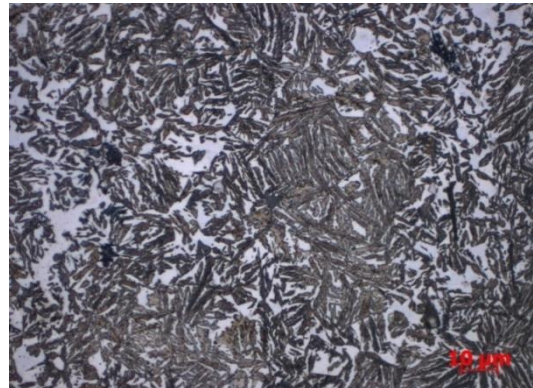


Fig. 7. Microstructure of ADI from C4 cycle. Etched with Beraha reagent - Martensite, 1000x. Pre-eutectoid ferrite, lower bainite, austenite

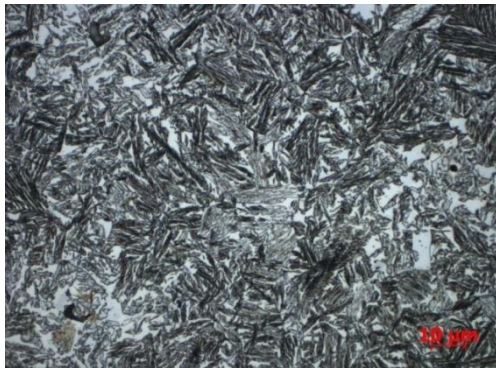


Fig. 8. Microstructure of ADI from C5 cycle. Etched with Beraha reagent - Martensite, 1000x. Pre-eutectoid ferrite, lower bainite, austenite

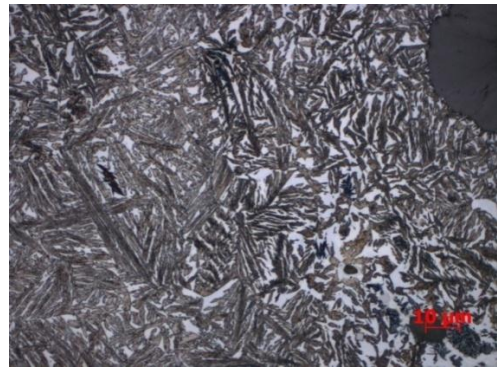


Fig. 9. Microstructure of ADI from C6 cycle. Etched with Beraha reagent - Martensite, 1000x. Pre-eutectoid ferrite, lower bainite, austenite

Model of results interpretation based on fuzzy logic

Technical limitations prevented obtaining in conducted experiments the amount of numerical results allowing their interpretation with statistical methods. Therefore, it was decided to use a more intuitive approach, which consisted in construction of a model based on the use of fuzzy logic, resulting next in the construction of rules governing the relationships between input and output parameters of the process investigated.

Output parameters are here the examined variants of heat treatment cycles determined by the values of variables used in the process of austenitising and austempering, summarised in Table 1.

The mechanical properties of ADI determined after heat treatment are compiled in Table 2. Among these properties, as output parameters for the fuzzy model, the yield strength YS and elongation EL have been selected.

As an additional input parameter, which in all the experiments has a constant value, the annealing time $t = 60$ minutes was adopted. Processing of these data was performed using MATLAB software, and a model of the structure shown in Figure 10 was obtained.

For each variable, appropriate membership functions were arbitrarily adopted, where central points corresponded to the values of parameters considered.

The runs of these functions for output variables, corresponding to different variants of the heat treatment, are shown in Figure 11, while Figure 12 illustrates the procedure for generating fuzzy rules defining the relationships between input and output parameters.

As a result of automatic interpretation of the rules, implemented in MATLAB system, visual representations of the occurring relationships were obtained, and they are presented in Figures 13, 14, and 15, respectively. Figure 13 illustrates a relationship between the yield strength YS and heat treatment conditions, while Figure 14 shows a relationship between the same parameters and the elongation EL. Figure 15 shows the same relationships in a slightly different perspective.

Attention deserves the fact that these visualisations cannot be used for drawing of conclusions of a quantitative nature (mainly due to the arbitrary choice of a membership function), but offer a general view on the nature of the existing relationships, and thus may serve as a guideline in seeking the most favourable (optimal) conditions for the implementation of the investigated heat treatment process.

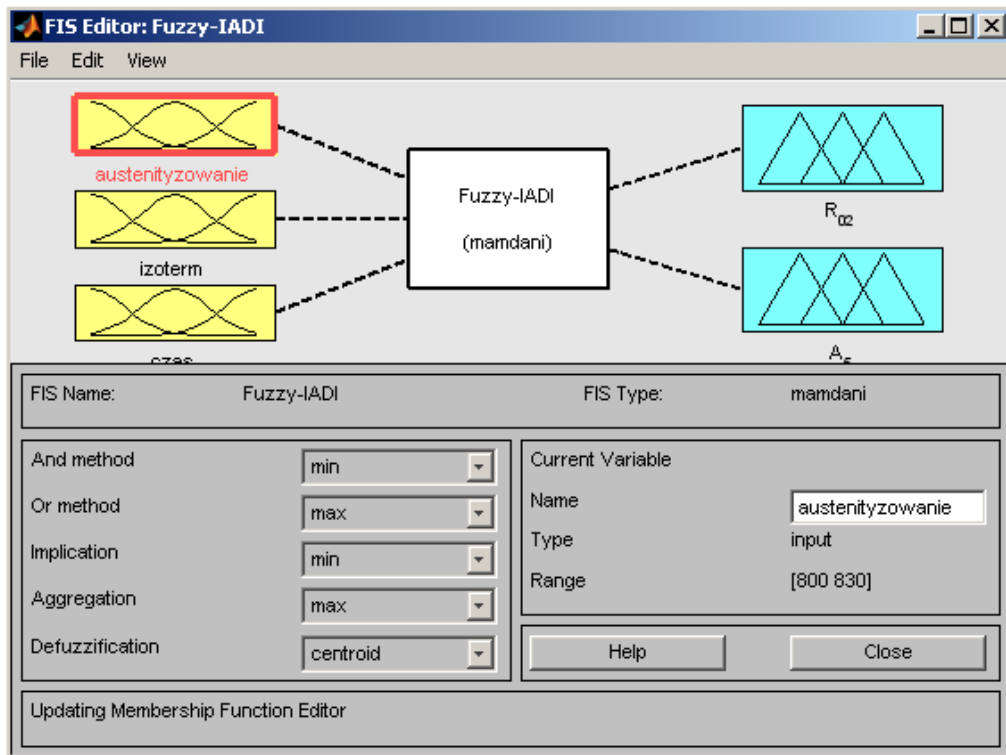


Fig. 10. Structure of Fuzzy Model

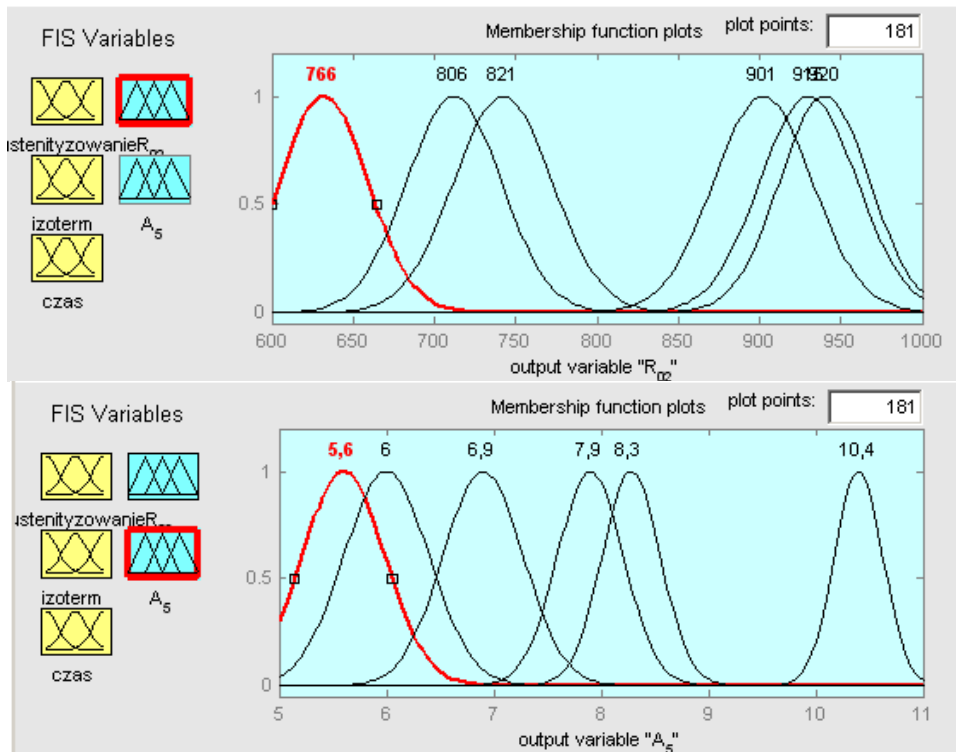


Fig. 11. The runs of the functions for output variables

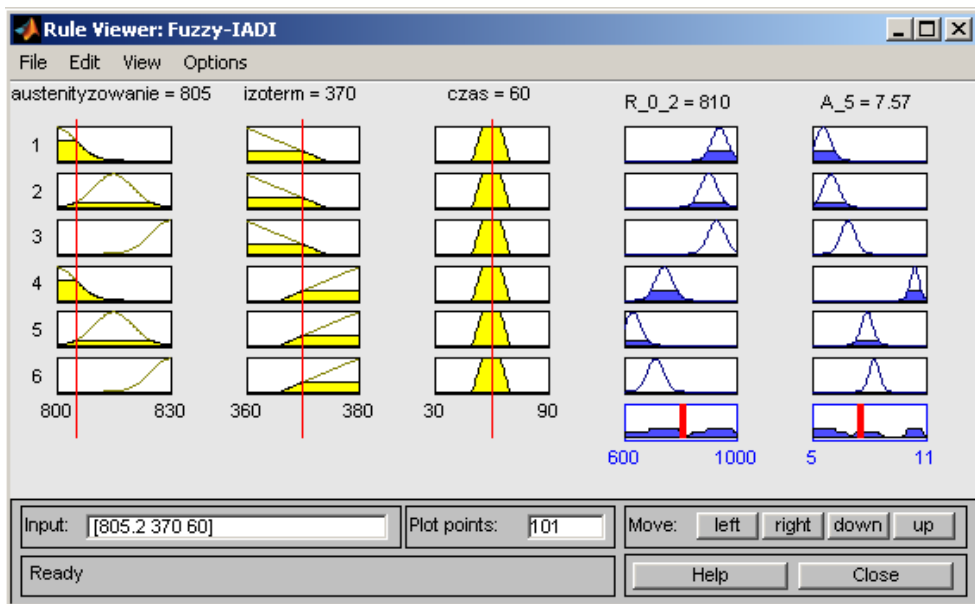


Fig. 12. Procedure for generating fuzzy rules

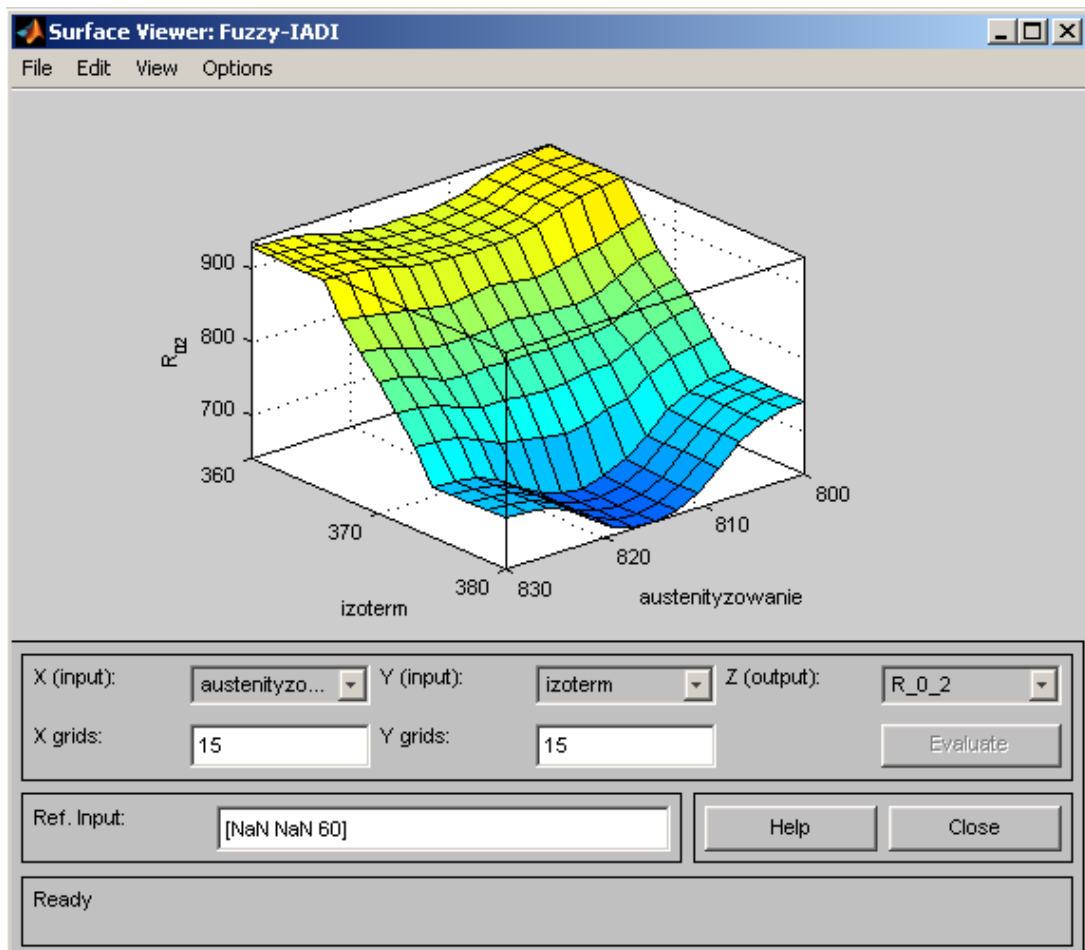


Fig. 13. Relationship between the yeild strength YS and heat treatment conditions

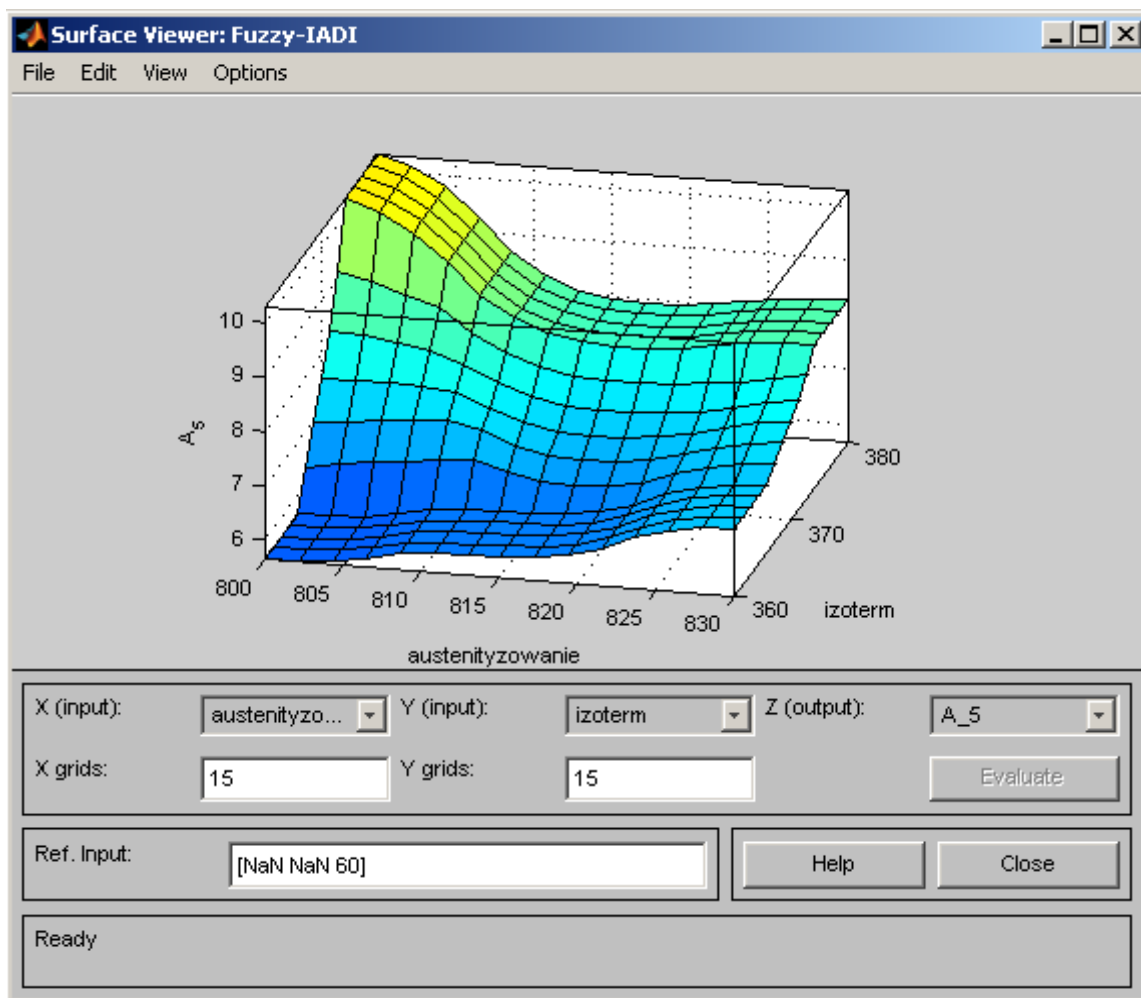


Fig. 14. Relationship between the elongation EL and heat treatment conditions

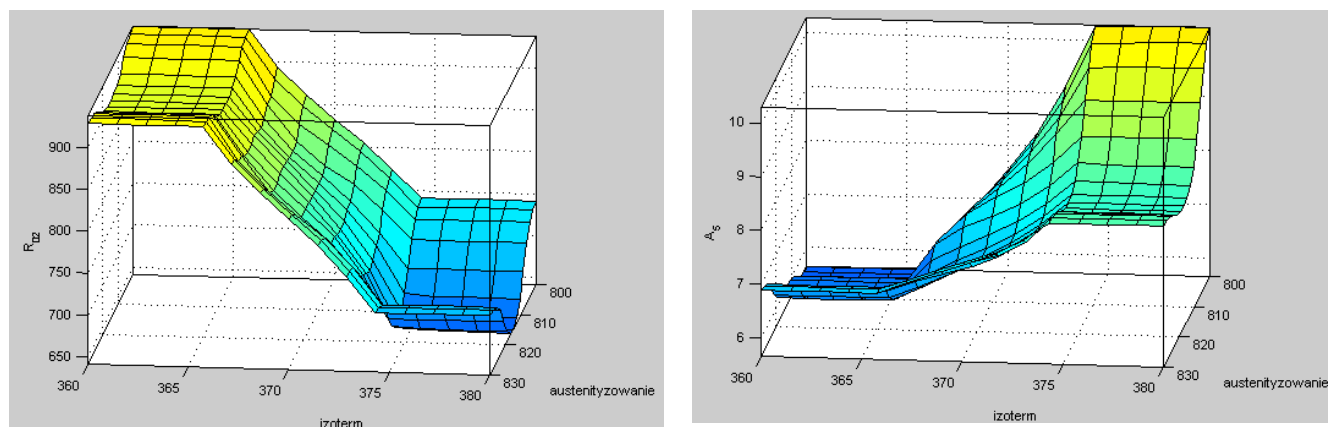


Fig. 15. Relationship between the yeild strength YS and elongation EL and heat treatment conditions at exchanged values of x and y axes

After partial austenitising, according to the assumptions adopted, certain amounts of pre-eutectoid ferrite were obtained in the cast iron matrix that caused an improvement of the mechanical properties (TS = 986 MPa, EL = 10.4, Hardness HRC = 34),

which is evident especially in cycle 4/6 (austenitising at 800⁰C, austempering at 380⁰C) with relatively high hardness, although higher content of eutectoid ferrite was expected in the matrix to give even better ductility. During studies it has been found that

this process is difficult to optimise, since it depends on both on the chemical composition and heat treatment parameters. Therefore, further studies are necessary in this respect.

4. Conclusions

1. Different variants of partial austenitising of the ductile iron containing 2.3% Si were applied.
2. Maximum content of pre-eutectoid ferrite in matrix, i.e. about 15%, was obtained after austenitising at 800°C and austempering at 380°C.
3. The obtained plastic properties of ADI are higher than the analogical properties demanded by PN EN 1564 for the 800-8 and 1000-5 grades.
4. Visualisation of the results using fuzzy logic module (in a MATLAB programme) gives no backgrounds for quantitative conclusions, but enables creating a general view about the character of the relationships and may serve as a guideline for further studies.

References

- [1] Girszowicz N.G. (1966). *Cristalisation and properties of cast iron in castings. (Kristalizacja i swojstwa czuguna w otliwkach)*. Maszynostrojenie, Moskwa – Leningrad 1966
- [2] Kovacs B. V. (1994). On the terminology and structure of ADI. *AFS Transactions*, 102, 417-420
- [3] Bayati H., Elliott R., Lorimer W. (1995). Influence of austenitising temperature on austempering kinetics of high manganese alloyed ductile cast iron. *Mat. Science and Technology*. 4(8), 776-771
- [4] Galarreta A., Boeri R.E., Sikora J.A. (1997). Free ferrite in pearlitic ductile iron - morphology and its influence on mechanical properties. *Cast Metals*. 9, 353-357
- [5] Aranzabal J., Serramoglia G., Rousière D. (2000) Development of a new mixed (ferritic-ausferritic) ductile iron for automotive suspension parts. *Metallurgical Science and Technology*. 18(1), 24-29
- [6] Rousière D., Aranzabal J. (1999). Obtention de structures mixtes dans le domaine des fontes à graphite sphéroïdal. *Hommes & fonderie*. 299(2), 18-22
- [7] Keyough J.R., Hayrynen K.L. (2003). Is it time for a grade 800 ADI in North America. *AFS Transactions*, 1-6
- [8] Kluska-Nawarecka S., Smolarek-Grzyb A., Wilk-Kołodziejczyk D., Adrian A. (2007). Knowledge Representation of Casting Metal Defects by Means of Ontology, *Archives of Foundry engineering, Polish Academy of Sciences*, e 7(3), 75-78. ISSN 1897-3310
- [9] Kluska-Nawarecka S., Górny Z., Wilk-Kołodziejczyk D., Smolarek-Grzyb A. (2007). The Logic of Plausible Reasoning in the Diagnosis of Castings Defects. *Archives of Metallurgy and Materials*. 52(3), 375-380, ISSN 1733-3490
- [10] F. Binczyk, A. Hanc, A. Kowalski. (2008). Austempering transformation kinetics of austempered ductile iron obtained by Mössbauer Spectroscopy. *Archives of Foundry Engineering*. 8(3), 15-21